

Supporting Information for

**Anion Dependence in Spin-Crossover Properties of a Fe(II) Podand Complex**

Christina M. Klug, Ashley M. McDaniel, Stephanie R. Fiedler, Brian S. Newell, and Matthew P. Shores

**Contents**

Figure S1. $^1\text{H}$ NMR spectrum of $\text{L}^{6\text{-OH}}$ in $\text{CD}_3\text{OD}$ at 400 MHz using TMS as the reference. ....	2
Figure S2. $^{13}\text{C}$ NMR spectrum of $\text{L}^{6\text{-OH}}$ in $\text{CD}_3\text{OD}$ , obtained on a 400 MHz NMR. ....	3
Figure S3. FT-IR spectrum of $\text{L}^{6\text{-OH}}$ obtained by pressing a solid sample on a ZnSe ATR crystal.....	3
Figure S4. $^1\text{H}$ NMR spectrum of $\text{L}^2$ in $\text{CDCl}_3$ at 400 MHz using $\text{CDCl}_3$ as the reference. ....	4
Synthesis of $[\text{FeL}^{6\text{-OH}}](\text{BPh}_4)_{1.75}\text{Br}_{0.25}\cdot\text{MeCN}$ (4a).....	4
Figure S5. $^{13}\text{C}$ NMR spectrum of $\text{L}^2$ in $\text{CDCl}_3$ , obtained on a 400 MHz NMR.....	5
Figure S6. FT-IR spectrum of $\text{L}^2$ obtained by pressing a solid sample using KBr salt plates.....	5
Figure S7. Variable temperature SQUID data for 4a.....	6
Figure S8. Variable temperature SQUID data for 2 and 2·0.5 MeOH.....	6
Figure S9. Crystal structure of 1·RT at 296 K.....	7
Figure S10. Crystal structure of 1·LT at 120 K. ....	7
Figure S11. Crystal structure of 2 at 120 K. ....	7
Figure S12. Crystal structure of 2·0.5 MeOH at 120 K. ....	8
Figure S13. Crystal structure of 3·RT at 296 K. ....	8
Figure S14. Crystal structure of 3·LT at 120 K. ....	8
Figure S15. Crystal structure of 4 at 120 K. ....	9
Figure S16. Crystal structure of 5 at 120 K.....	9
Table S1. Shortest intermolecular hydrogen-bond interactions. <sup>a</sup> .....	10
Figure S17. Packing plot of 2 down the <i>a</i> axis.....	11
Figure S18. Packing plot of 2 down the <i>b</i> axis. ....	11
Figure S19. Packing plot of 2·0.5 MeOH down the <i>b</i> axis. ....	12
Figure S20. Intermolecular interactions for the structures of compound 3·LT.....	12
Figure S21. Anion-cation interactions of 1·RT.....	13
Figure S22. Anion-cation and cation-cation interactions of 1·LT. ....	13
Figure S23. Intermolecular interactions of 4. ....	14
Figure S24. Cation-anion interactions for 5.....	14
Figure S25. $^1\text{H}$ NMR spectra obtained at 295 K of 2.....	15
Figure S26. $^1\text{H}$ NMR spectra obtained at 295 K of 5.....	16

Figure S27.  $^1\text{H}$  NMR spectra of 2 (normal/diamagnetic window) before (top) and after (bottom) addition of 3 equivalents of 2,2'-bipyridine. .... 17

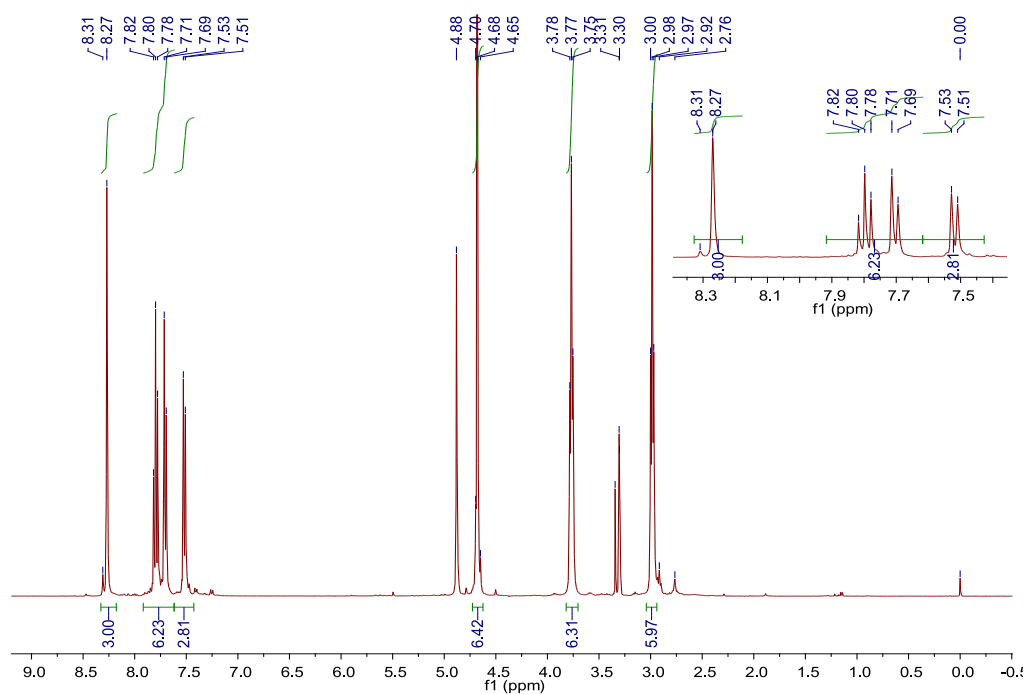
Figure S28.  $^1\text{H}$  NMR spectra of 2 (wider window) before (top) and after (bottom) addition of 3 equivalents of 2,2'-bipyridine. .... 17

Figure S30.  $^1\text{H}$  NMR spectra of 5 (wider window) before (top) and after (bottom) addition of 3 equivalents of 2,2'-bipyridine. .... 19

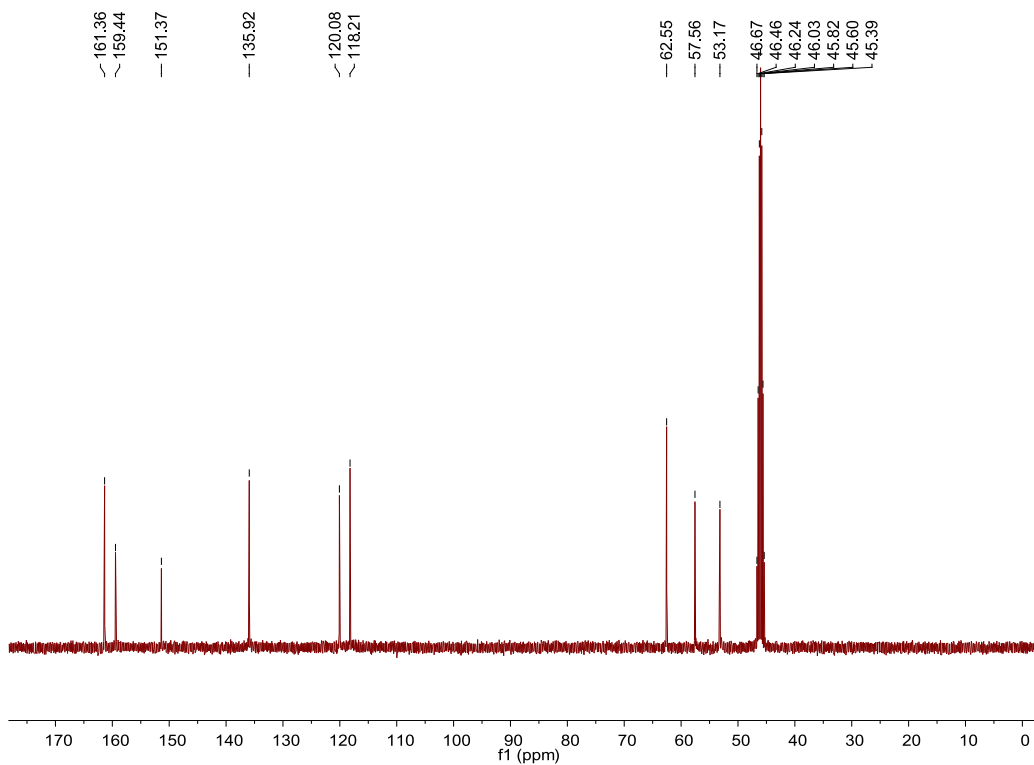
Figure S31.  $^1\text{H}$  NMR spectra of 1 at 295 K (top) and 213 K (middle and bottom) ..... 20

Figure S32.  $^1\text{H}$  NMR spectra of 1 at 298 K (top) and 193 K (bottom) ..... 21

Figure S33. Variable temperature solution magnetic susceptibility of 1, 2, 3 and 5 in  $\text{CD}_3\text{OD}$  using Evans' method. .... 22



**Figure S1.**  $^1\text{H}$  NMR spectrum of  $\text{L}^{6-\text{OH}}$  in  $\text{CD}_3\text{OD}$  at 400 MHz using TMS as the reference.



**Figure S2.**  $^{13}\text{C}$  NMR spectrum of  $\text{L}^{6\text{-OH}}$  in  $\text{CD}_3\text{OD}$ , obtained on a 400 MHz NMR. Multiplet at 46 ppm is  $\text{CD}_3\text{OD}$ .

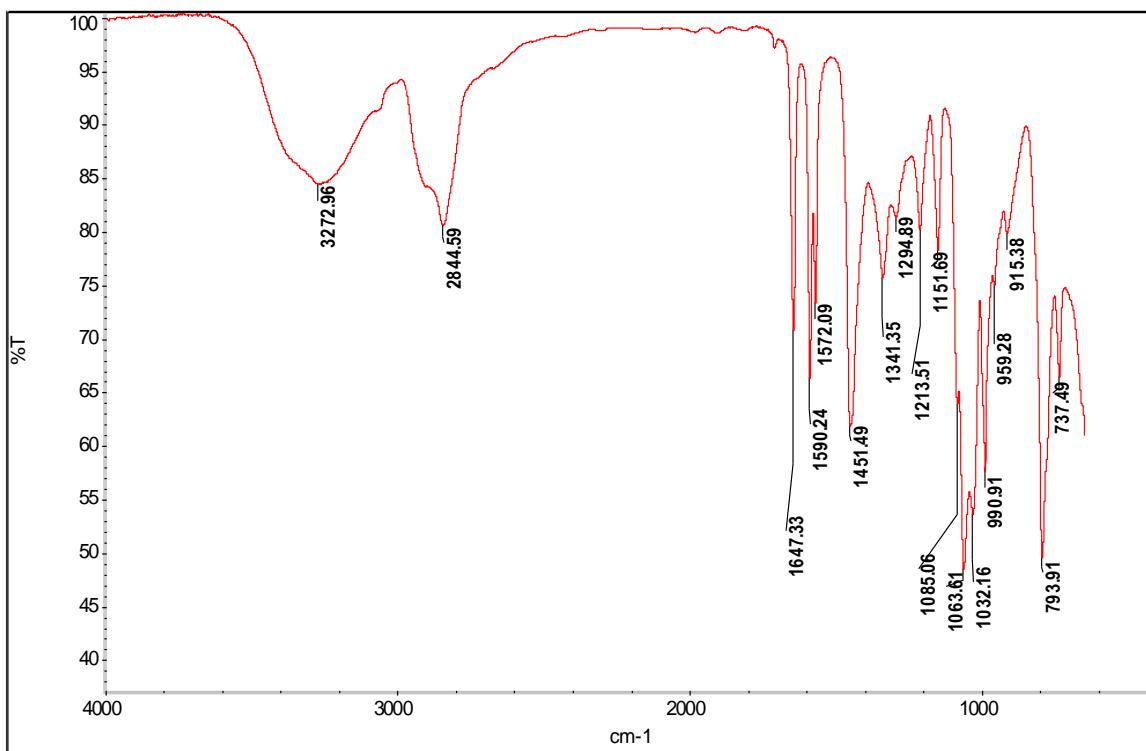


**Figure S3.** FT-IR spectrum of  $\text{L}^{6\text{-OH}}$  obtained by pressing a solid sample on a ZnSe ATR crystal.

### Synthesis of $[\text{FeL}^{6\text{-OH}}](\text{BPh}_4)_{1.75}\text{Br}_{0.25}\cdot\text{MeCN}$ (**4a**)

Carried out in a manner similar to the preparation of **3**, anion exchange of **2** (0.073 g, 0.102 mmol) into 6 mL of methanol with  $\text{NaBPh}_4$  (0.140 g, 0.409 mmol) produced a light pink precipitate. The mixture was stirred for an additional 30 minutes, and then the solid was isolated by filtration. The resulting residue was triturated with methanol ( $2 \times 6$  mL) and 6 mL of  $\text{Et}_2\text{O}$  to produce a brick red, free flowing powder. Crystals were obtained by  $\text{Et}_2\text{O}$  diffusion into a concentrated acetonitrile solution (0.069 g, 58 % yield); X-ray quality crystals were not obtained by this method. IR (ATR)  $\nu_{\text{OH}}$   $3509\text{ cm}^{-1}$ .  $\lambda_{\text{max}}$  (MeCN)/nm 489 ( $1340\text{ M}^{-1}\cdot\text{cm}^{-1}$ ).  $^1\text{H NMR}$  ( $\text{CD}_3\text{CN}$ )  $\delta$  75.3, 56.9, 47.9, 40.7, 32.3, 10.4, 8.9 ppm.  $\chi_{\text{M}}T$  (SQUID, 296 K) =  $3.62\text{ cm}^3\text{ K mol}^{-1}$  ( $\mu_{\text{eff}} = 5.38\ \mu_{\text{B}}$ ). Anal. Calcd for  $\text{C}_{71}\text{H}_{71}\text{N}_8\text{O}_3\text{Fe B}_{1.75}\text{Br}_{0.25}$ : C, 72.3; H, 6.1 N, 9.5. Found: C, 72.3; H, 6.0; N, 9.1.

The magnetic behaviour of the mixed anion salt **4a** is distinct from what one might expect from a mixture of **2** and “[ $\text{FeL}^{6\text{-OH}}](\text{BPh}_4)_2$ ” in that no distinct SCO is observed at ca. 100 K. Instead  $\chi_{\text{M}}T$  for **4** is  $3.62\text{ cm}^3\text{ K mol}^{-1}$  at 295 K, and slowly decreases to  $2.21\text{ cm}^3\text{ K mol}^{-1}$  by 15 K. The sharp downturn in  $\chi_{\text{M}}T$  to  $1.66\text{ cm}^3\text{ K mol}^{-1}$  at 5 K is ascribed to zero-field splitting in the residual HS fraction. The microscopic origins of the unique spin-state behaviour for this compound are unknown, as structural analysis has not been performed on this compound.

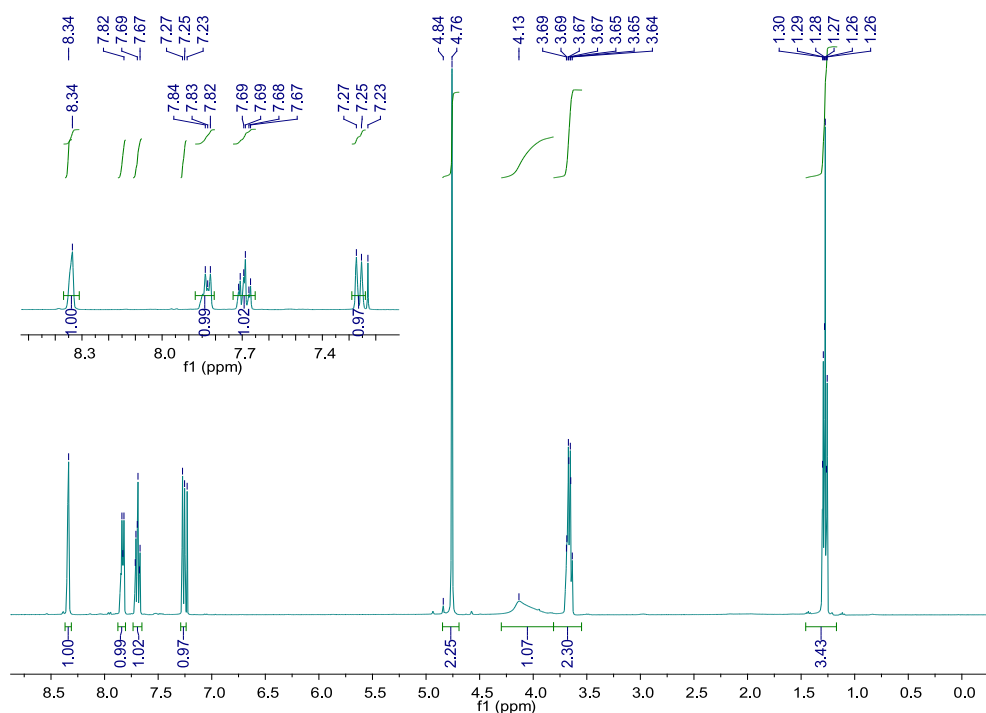


**Figure S4.**  $^1\text{H NMR}$  spectrum of  $\text{L}^2$  in  $\text{CDCl}_3$  at 400 MHz using  $\text{CDCl}_3$  as the reference.

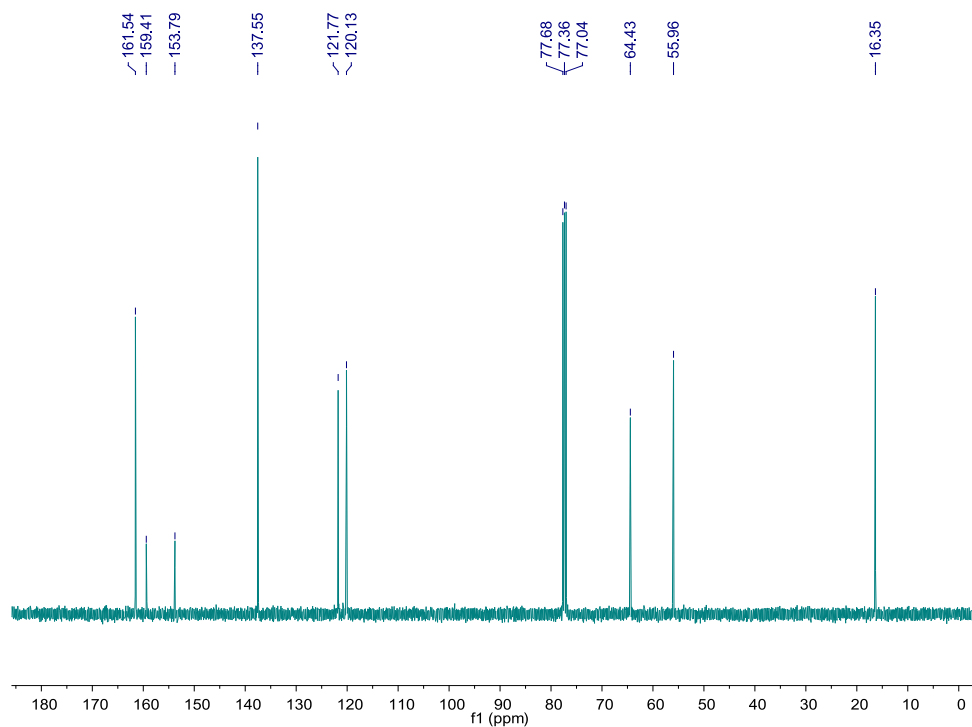


**Figure S5.**  $^{13}\text{C}$  NMR spectrum of  $\text{L}^2$  in  $\text{CDCl}_3$ , obtained on a 400 MHz NMR. Multiplet at 77 ppm is  $\text{CDCl}_3$ .

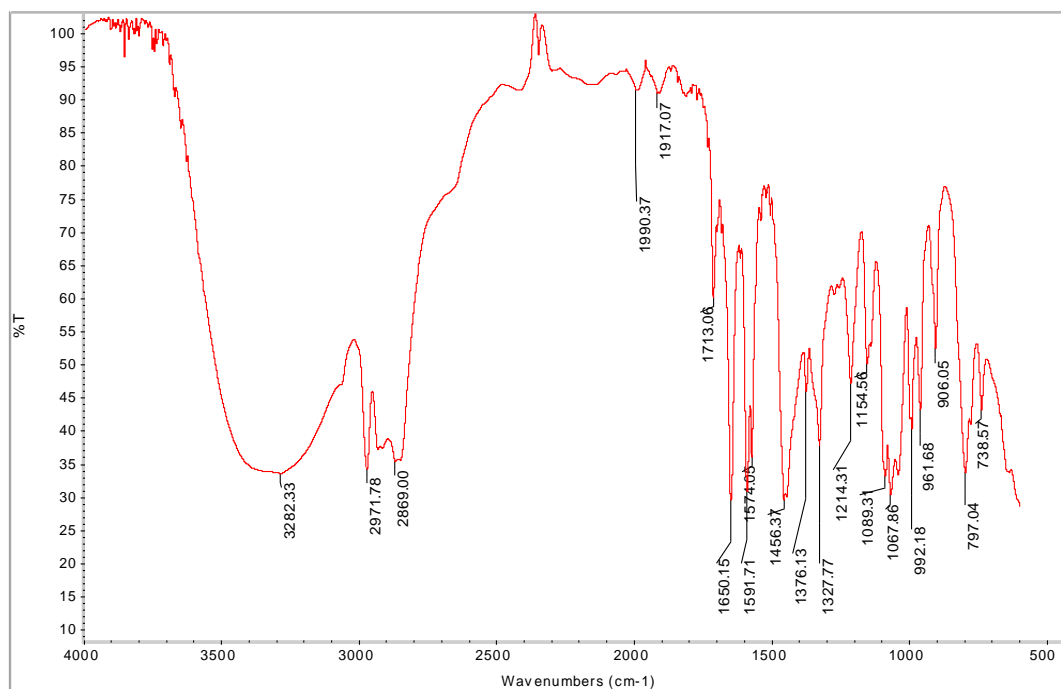


**Figure S6.** FT-IR spectrum of  $\text{L}^2$  obtained by pressing a solid sample using KBr salt plates.

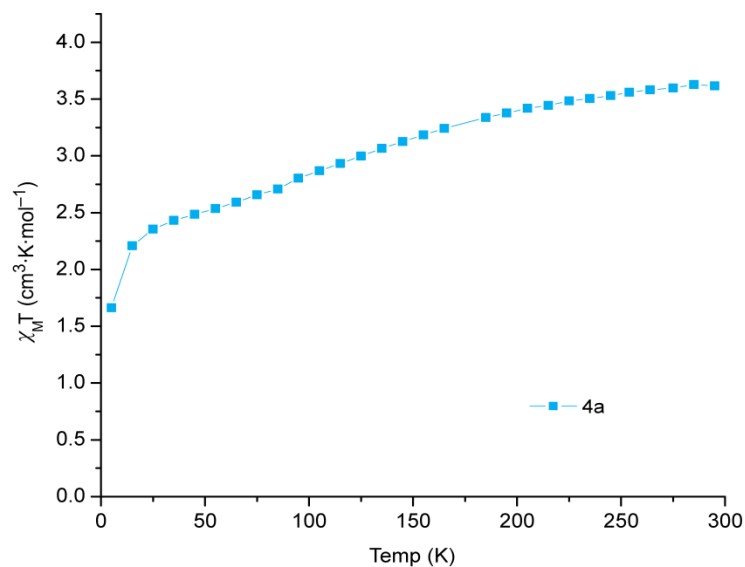


**Figure S7.** Variable temperature SQUID data for **4a**.

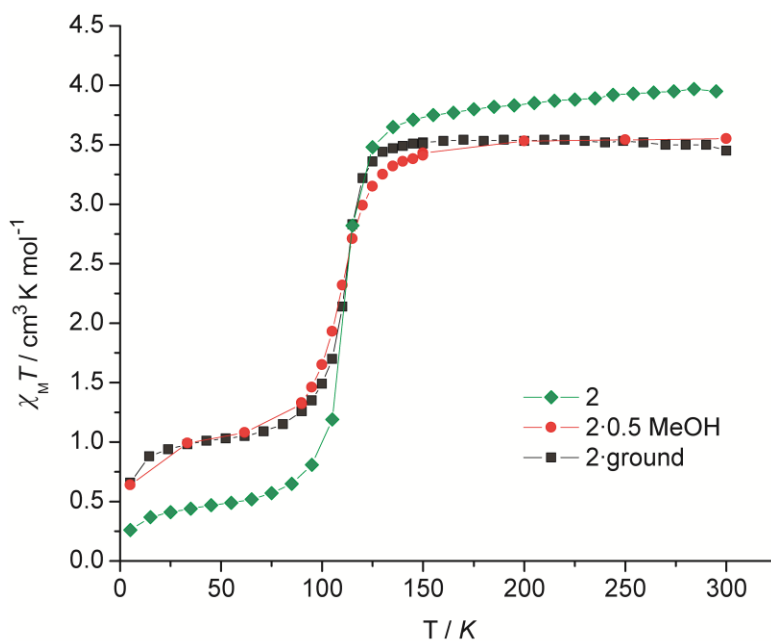


**Figure S8.** Variable temperature SQUID data for **2** and **2·0.5 MeOH**. Samples **2** and **2·ground** differ only in the amount of grinding applied to the crystals (**2·ground** was ground more vigorously than **2**).

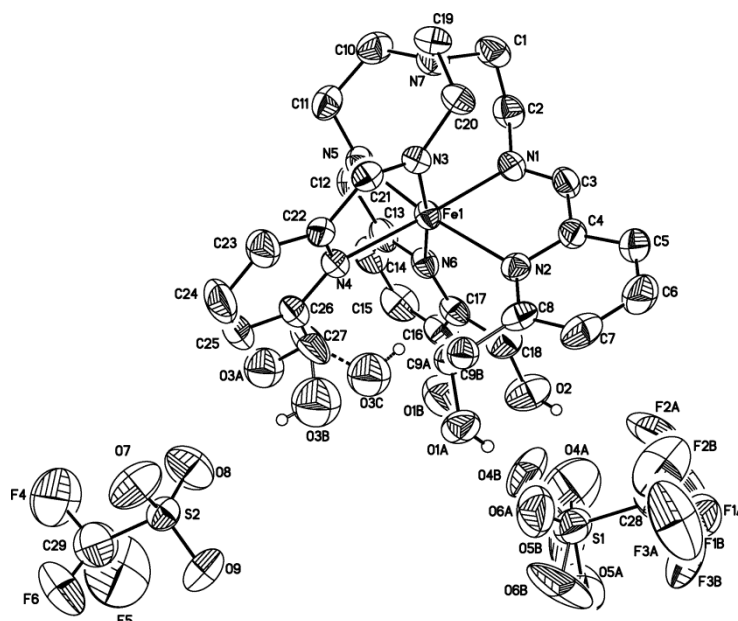


**Figure S9.** Crystal structure of **1-RT** at 296 K. Atoms rendered with 40% thermal ellipsoids. Hydrogen atoms except those of the hydroxyls have been omitted for clarity.

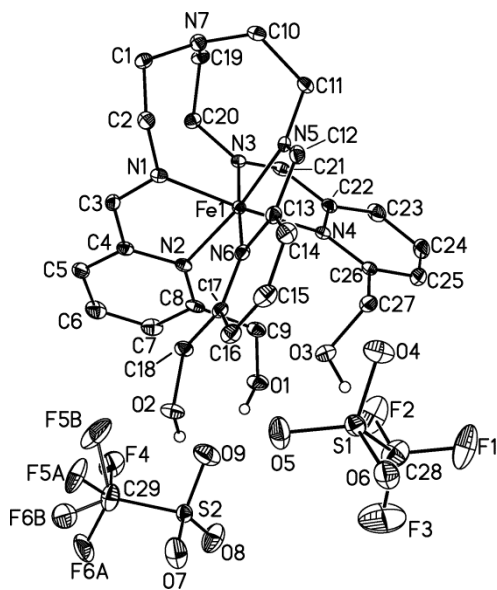


**Figure S10.** Crystal structure of **1-LT** at 120 K. Atoms rendered with 40% thermal ellipsoids. Hydrogen atoms except those of the hydroxyls have been omitted for clarity.

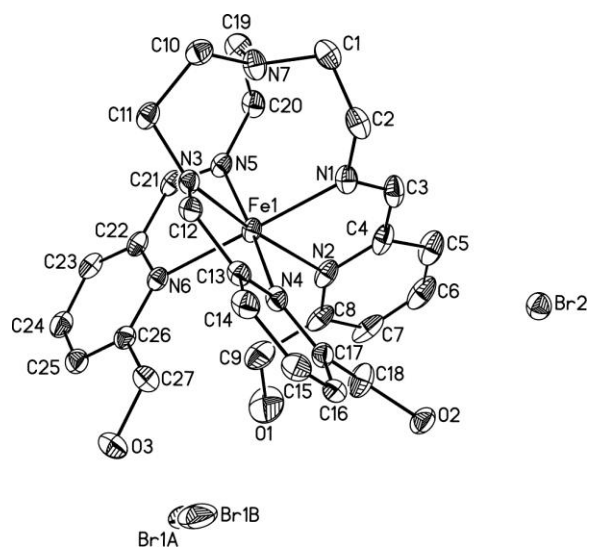


**Figure S11.** Crystal structure of **2** at 120 K. Atoms rendered with 40% thermal ellipsoids. Hydrogen atoms have been omitted for clarity.

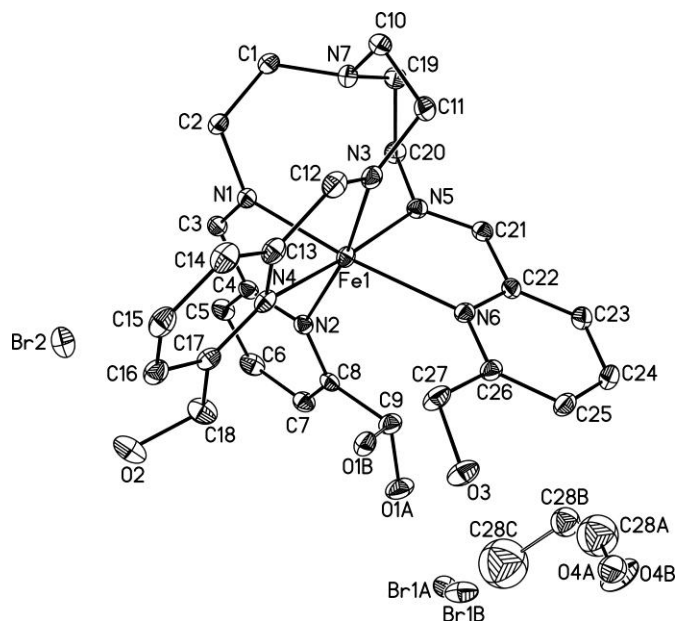


**Figure S12.** Crystal structure of **2·0.5 MeOH** at 120 K. Hydrogen atoms have been removed for clarity. Atoms rendered with 40% thermal ellipsoids. Solvent molecules (C28a, C28b, C28c, O4a and O4b) were refined isotropically due to high level of disorder.

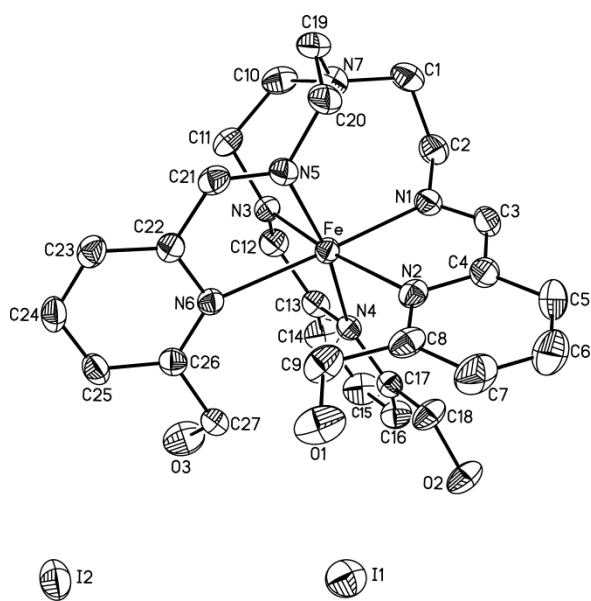


**Figure S13.** Crystal structure of **3·RT** at 296 K. Atoms rendered with 40% thermal ellipsoids. Hydrogen atoms have been omitted for clarity.

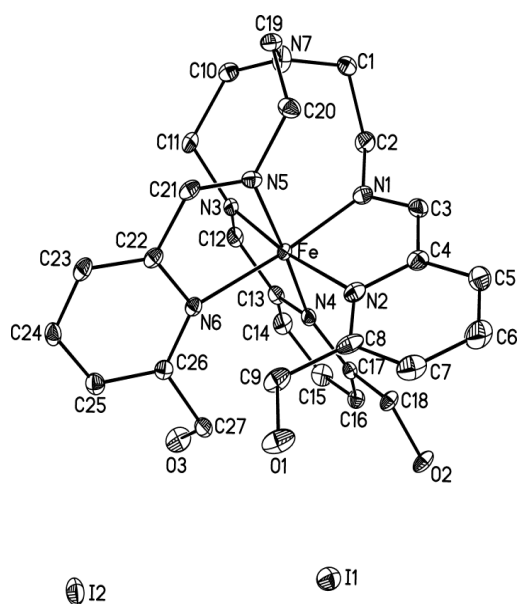


**Figure S14.** Crystal structure of **3·LT** at 120 K. Atoms rendered with 40% thermal ellipsoids. Hydrogen atoms except those of the hydroxyls have been omitted for clarity.



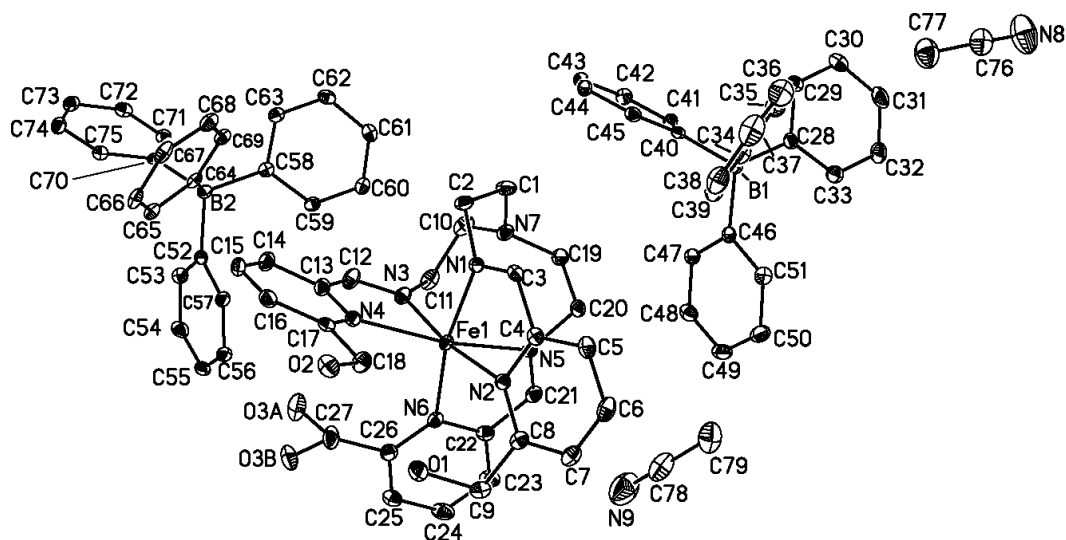


**Figure S15.** Crystal structure of **4** at 120 K. Atoms rendered with 40% thermal ellipsoids. Hydrogen atoms have been omitted for clarity.

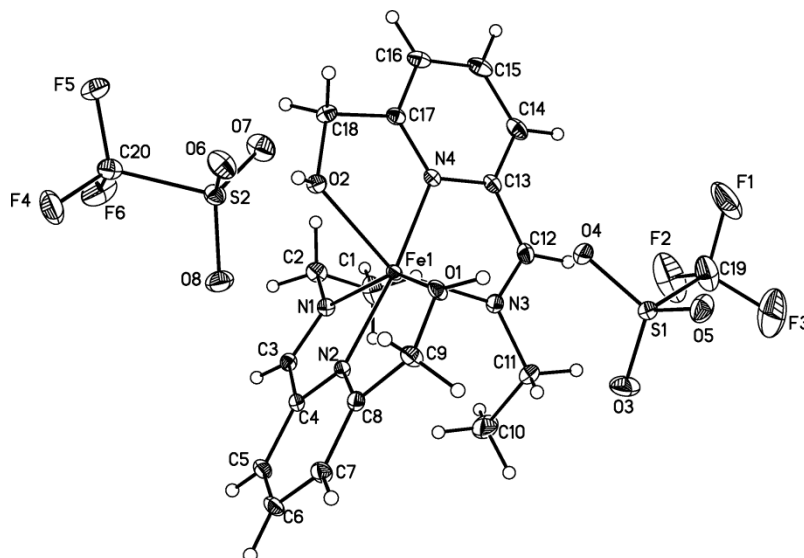


**Figure S16.** Crystal structure of **5** at 120 K. Atoms rendered with 40% thermal ellipsoids.

**Table S1.** Shortest intermolecular hydrogen-bond interactions.<sup>a</sup>

	<b>1·RT</b>	<b>1·LT</b>	<b>2</b>	<b>2·0.5 MeOH</b>	<b>3·RT</b>	<b>3·LT</b>	<b>4</b>	<b>5</b>
O1...X1 <sup>b</sup>	2.58(1) <sup>c</sup>	2.813(3) <sup>d</sup>	3.354(8)	3.22(4)	3.410(2)	3.360(2)	–	2.636(1)
O2...X1	2.68(1) <sup>c</sup>	2.964(3) <sup>d</sup>	3.203(7)	3.277(6)	4.037(2)	3.888(2)	3.154(7) <sup>e</sup>	2.610(1)
O3...X2	2.83(2)	–	3.224(3)	3.213(2)	3.599(2)	3.596(2)	3.326(13) <sup>e</sup>	–
O3...N7	4.40(9)	2.827(3)	–	–	–	–	–	–
O1...O2a	–	–	–	–	2.743(3)	2.705(3)	2.742(2)	–

<sup>a</sup> Interaction defined as distance less than the sum of the van der Waals radii: (O...O = 3.04 Å, O...Br = 3.37 Å, O...I = 3.50 Å, O...N = 3.02 Å; taken from "Atomic Radii of the Elements," in CRC Handbook of Chemistry and Physics, 92nd Edition (Internet Version 2012), W. M. Haynes, ed., CRC Press/Taylor and Francis, Boca Raton, FL.)

<sup>b</sup> X1 is defined as 'anion 1' (lies closest to the trigonal pocket), X2 is defined as 'anion 2' (See renderings/packing plots).

<sup>c</sup> Interact with two different oxygen atoms of triflate

<sup>d</sup> Interact with same oxygen atom of triflate

<sup>e</sup> Defined as the distance between the centroid of the phenyl and the oxygen

Variations on the anion chelation are seen between **1·RT** and **1·LT**: at room temperature, the two chelating arms bind with two oxygen atoms of the triflate; while at 120 K, the two arms interact with only one oxygen atom (Figure 5 in the manuscript).

In the structures of **3**, we note that the two arms of the iodide-containing structures do not interact with the anion equally, as denoted by significantly different O...I distances.

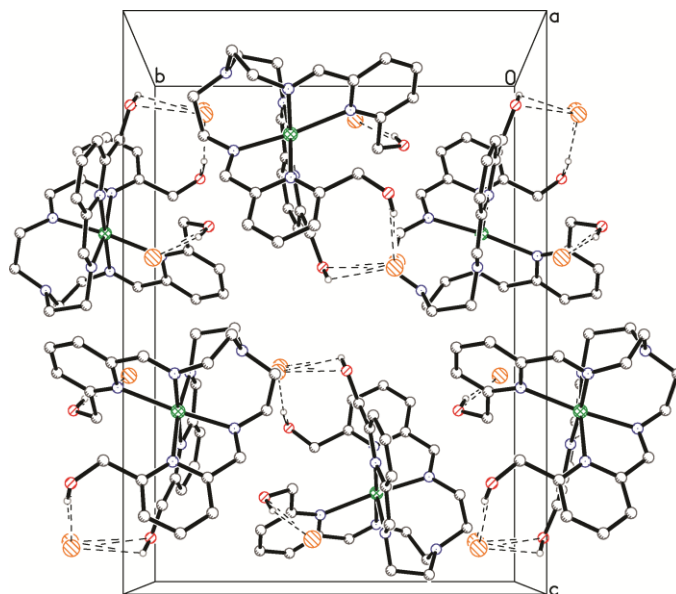


**Figure S17.** Packing plot of **2** down the *a* axis. Fe, C, N, O, H and Br atoms are colored green, dark gray, blue, red, light gray and orange respectively. Dashed bonds are to emphasize hydrogen bonding interactions.

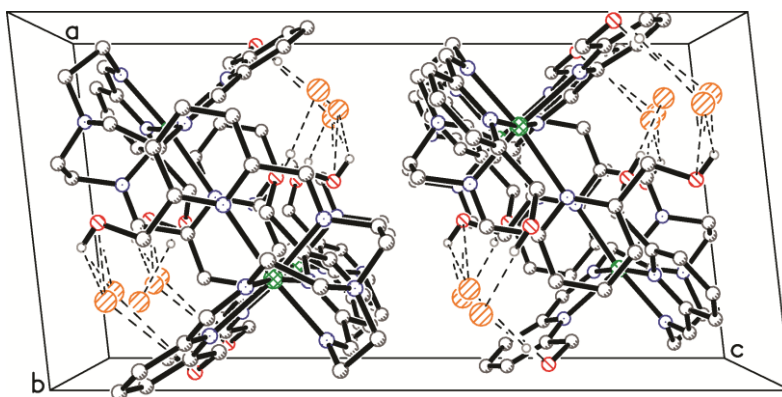


**Figure S18.** Packing plot of **2** down the *b* axis. Fe, C, N, O, H and Br atoms are colored green, dark gray, blue, red, light gray and orange respectively. Dashed bonds are to emphasize hydrogen bonding interactions.

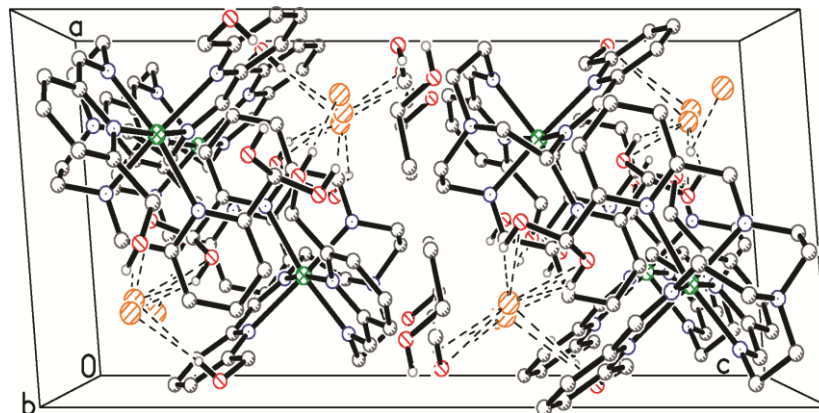


**Figure S19.** Packing plot of  $2 \cdot 0.5 \text{ MeOH}$  down the  $b$  axis. Fe, C, N, O, H and Br atoms are colored green, dark gray, blue, red, light gray and orange respectively. Dashed bonds are to emphasize hydrogen bonding interactions.

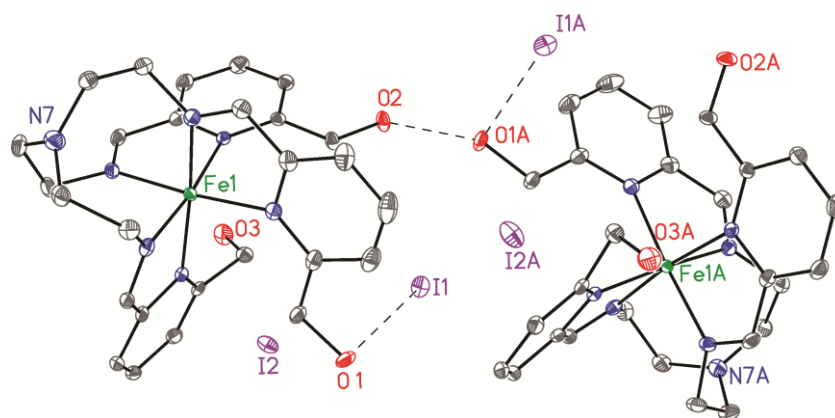


**Figure S20.** Intermolecular interactions for the structures of compound  $3 \cdot \text{LT}$ . Analogous interactions are seen at 296 and 120 K. Atoms rendered with 40% thermal ellipsoids. Fe, C, N, O and I atoms are colored green, dark gray, blue, red and purple respectively. Hydrogen atoms have been omitted for clarity.

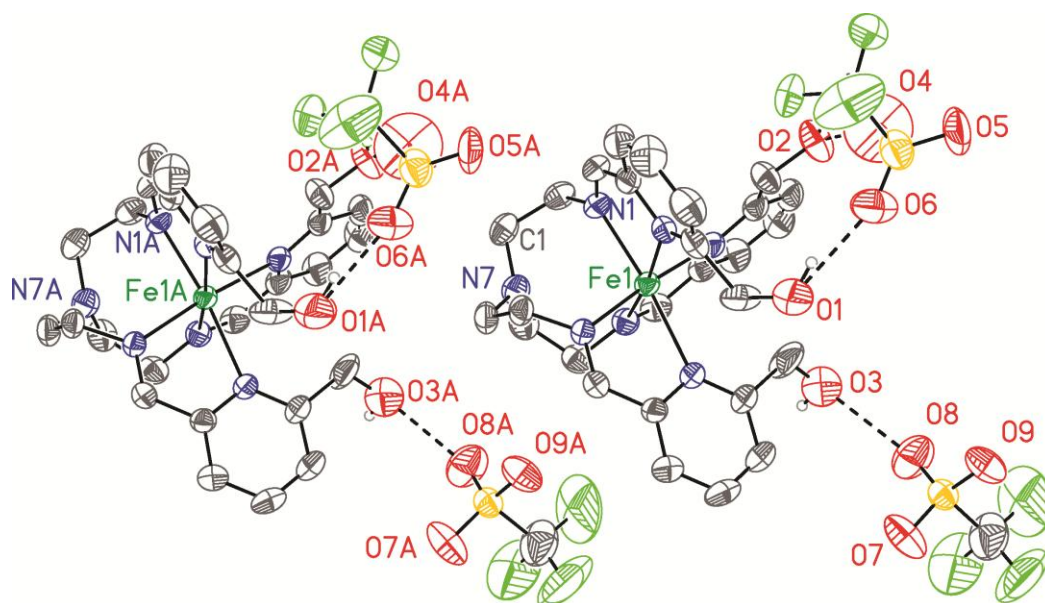


**Figure S21.** Anion-cation interactions of **1·RT**. Atoms rendered with 40% thermal ellipsoids. Fe, C, N, O, S and F atoms are colored dark green, dark gray, blue, red, yellow and light green respectively. Hydrogen atoms except those of the hydroxyls have been omitted for clarity.

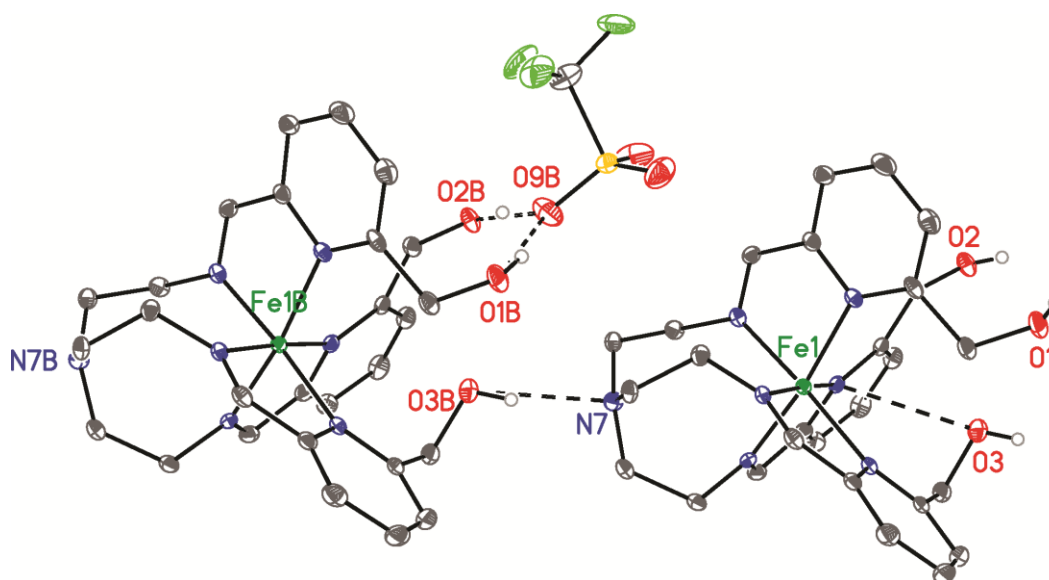


**Figure S22.** Anion-cation and cation-cation interactions of **1·LT**. Fe, C, N, O, S and F atoms are colored dark green, dark gray, blue, red, yellow and light green respectively. Hydrogen atoms except those of the hydroxyls have been omitted for clarity.

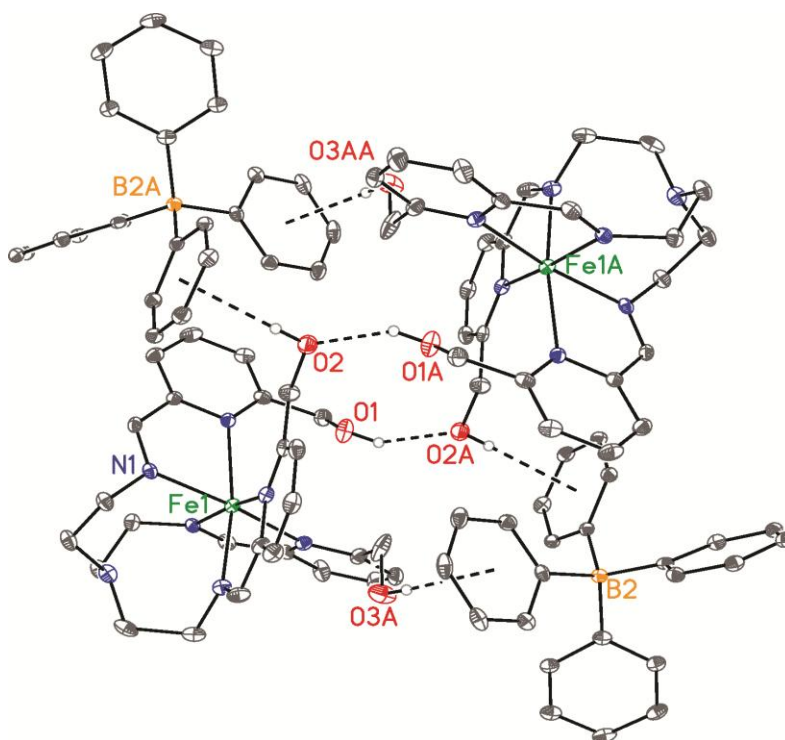


**Figure S23.** Intermolecular interactions of **4**. Fe, C, N, O, and B atoms are colored dark green, dark gray, blue, red, and yellow respectively. Hydrogen atoms except those of the hydroxyls and disorder of O3 have been omitted for clarity.

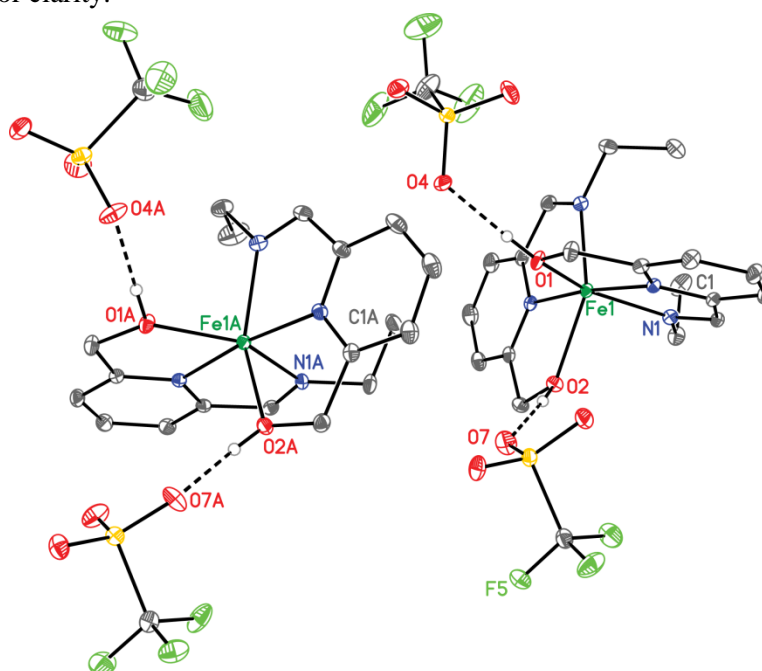


**Figure S24.** Cation-anion interactions for **5**. Fe, C, N, O, S and F atoms are colored dark green, dark gray, blue, red, yellow and light green respectively. Hydrogen atoms except those of the hydroxyls have been omitted for clarity.

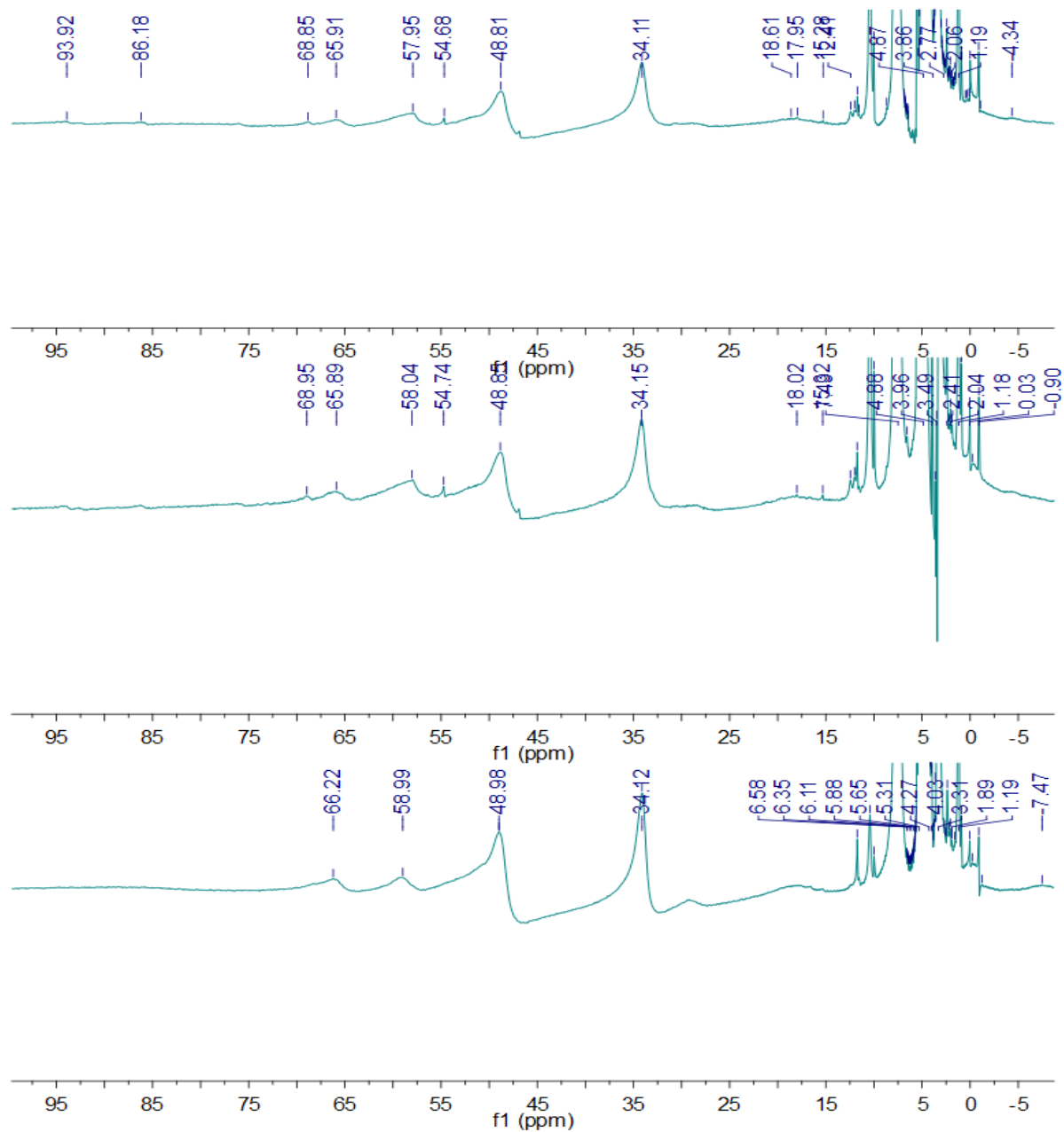


**Figure S25.**  $^1\text{H}$  NMR spectra obtained at 295 K at 300 MHz with TMS as the reference of **2** at  $t=10$  min. (bottom),  $t=24$  hr (middle) and  $t=3$  days (top). After 24 hours, additional peaks begin to appear at 54.7, 68.9, 86.2 and 93.9 ppm indicative of complex degradation.

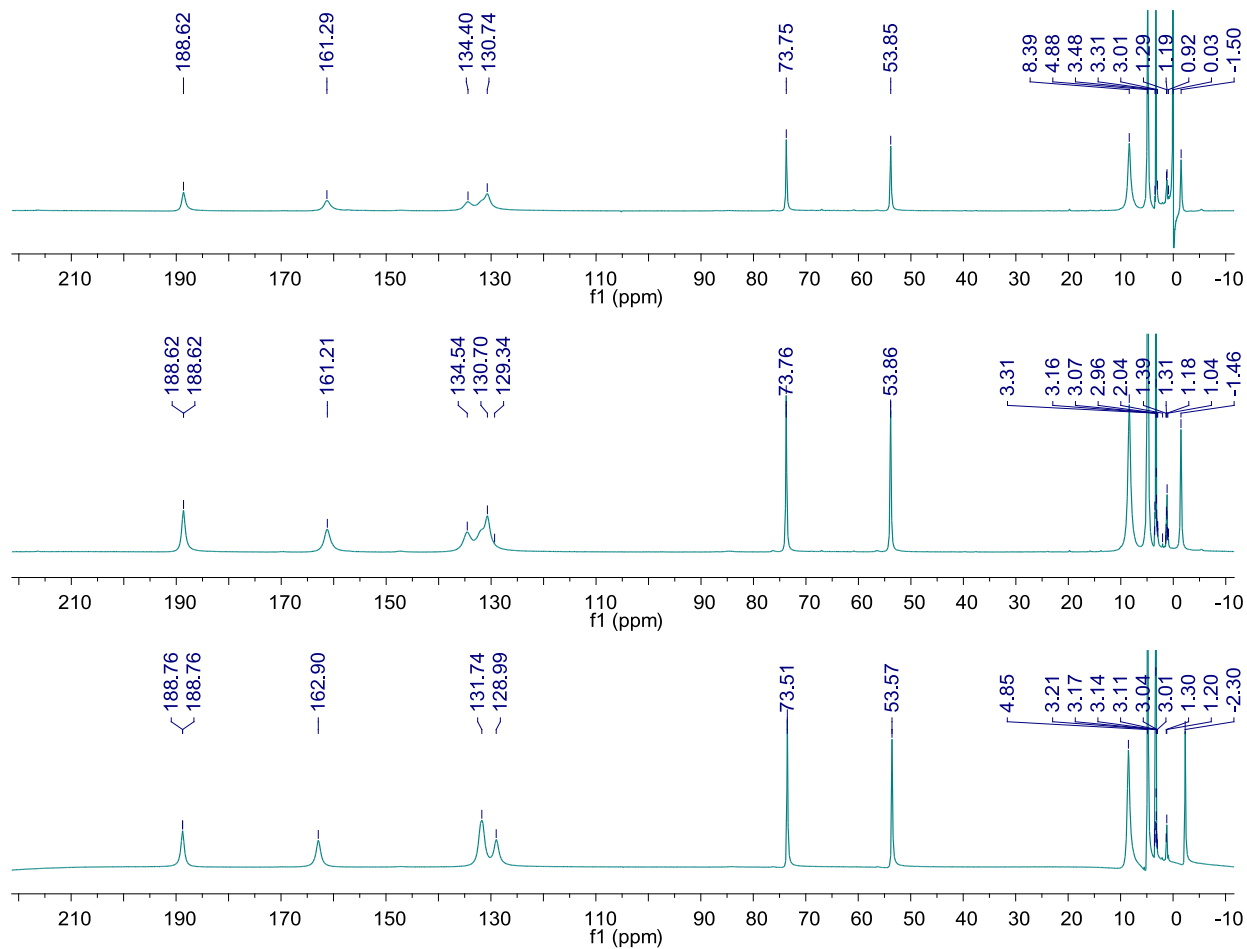


**Figure S26.**  $^1\text{H}$  NMR spectra obtained at 295 K at 300 MHz with  $\text{CD}_3\text{OD}$  as the reference of **5** at  $t=10$  min. (bottom),  $t=1$  day (middle) and  $t=3$  days (top). Shifts in some peaks and the growth of small resonances are seen over time.



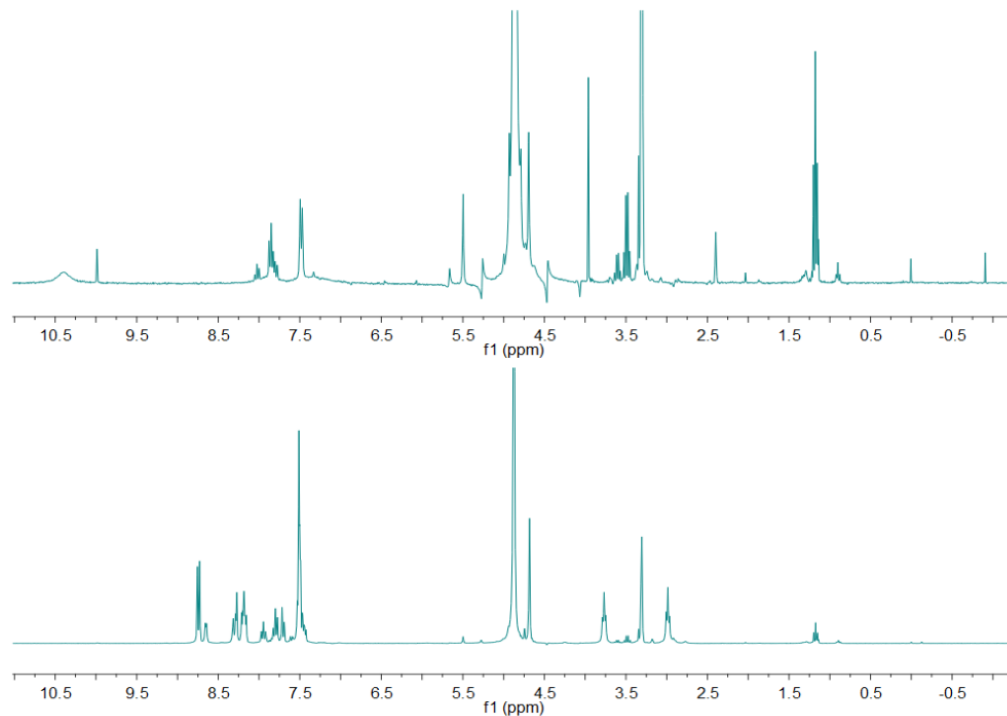


**Figure S27.**  $^1\text{H}$  NMR spectra of **2** (normal/diamagnetic window) before (top) and after (bottom) addition of 3 equivalents of 2,2'-bipyridine. NMR spectra obtained at 295 K at 300 MHz with TMS reference.

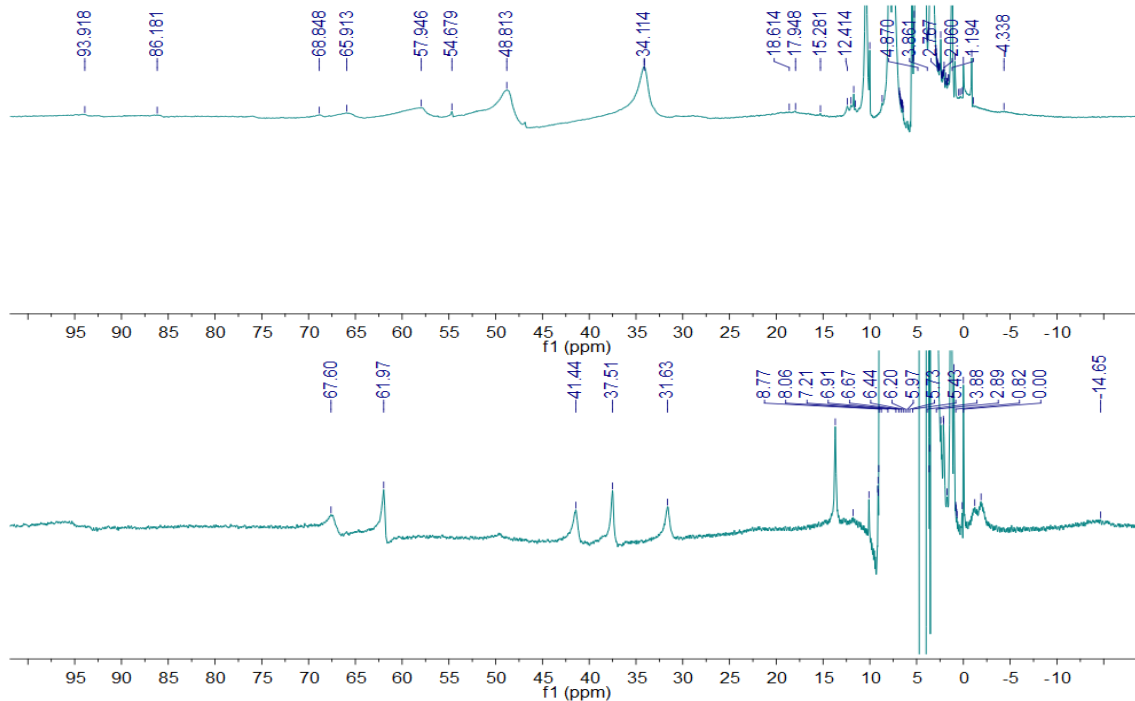


**Figure S28.**  $^1\text{H}$  NMR spectra of **2** (wider window) before (top) and after (bottom) addition of 3 equivalents of 2,2'-bipyridine. NMR spectra obtained at 295 K at 300 MHz with TMS as the reference.

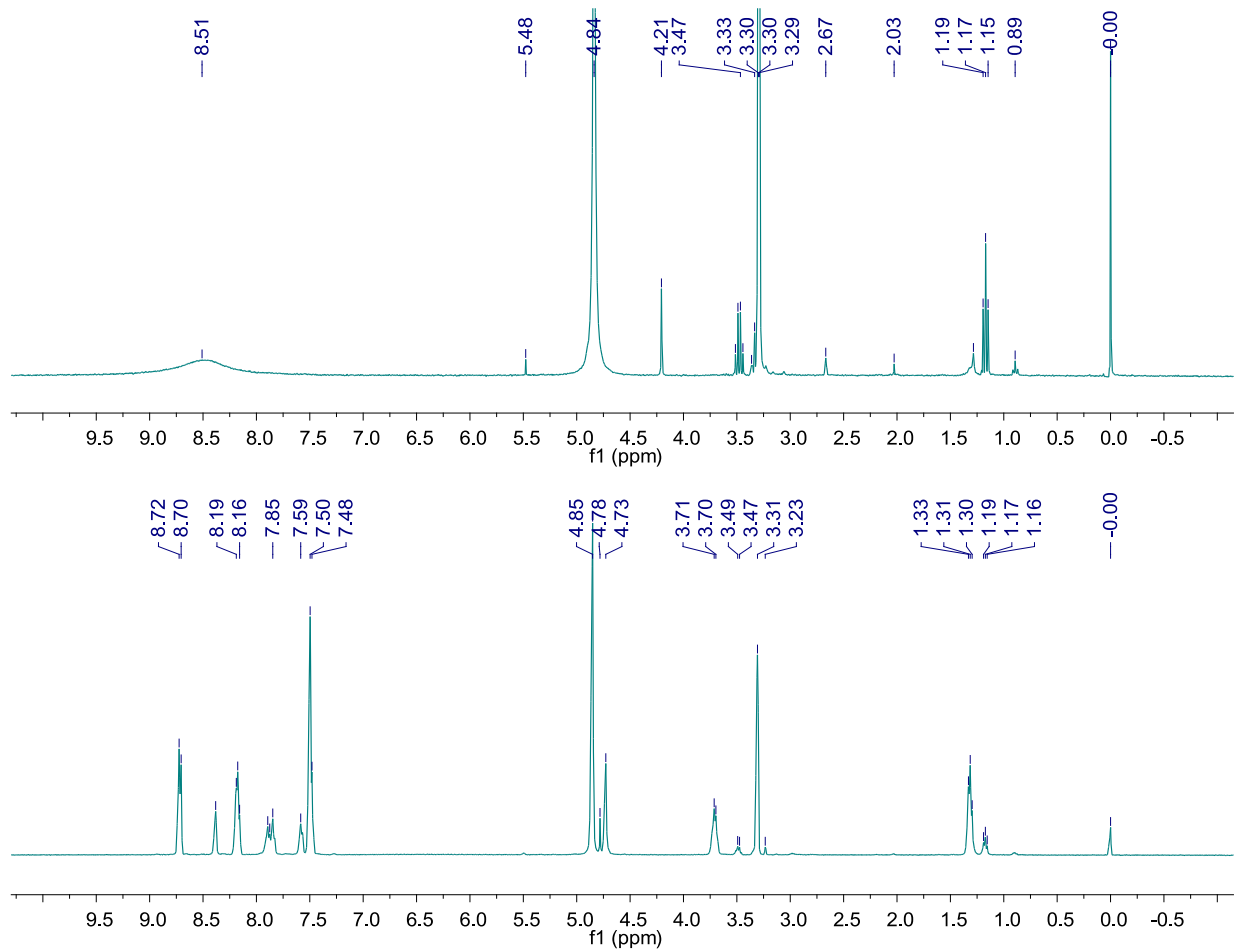


**Figure S29.** <sup>1</sup>H NMR spectra of **5** (normal/diamagnetic window) before (top) and after (bottom) addition of 3 equivalents of 2,2'-bipyridine. NMR spectra obtained at 295 K at 300 MHz with TMS reference.

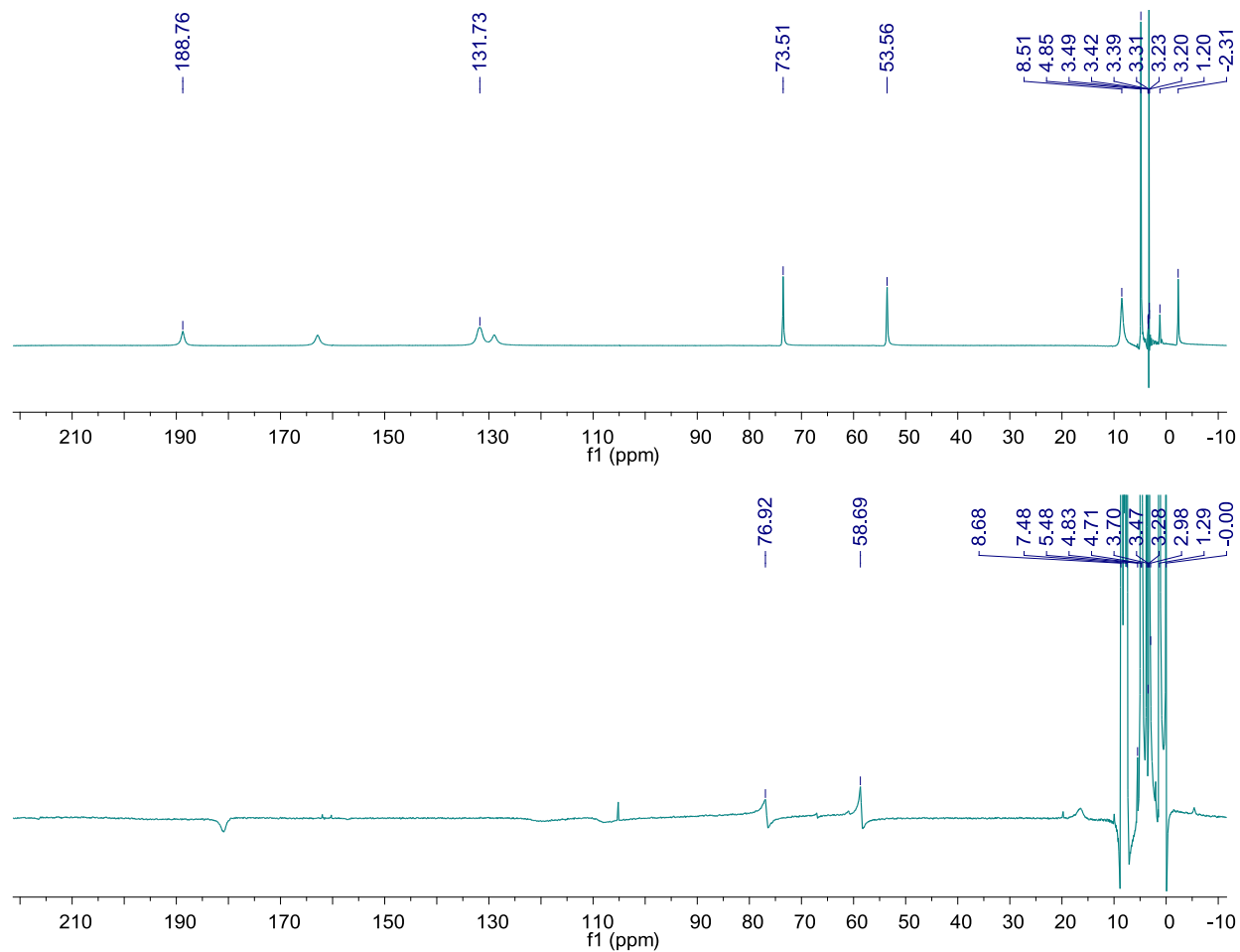


**Figure S30.** <sup>1</sup>H NMR spectra of **5** (wider window) before (top) and after (bottom) addition of 3 equivalents of 2,2'-bipyridine. NMR spectra obtained at 295 K at 300 MHz with TMS reference.

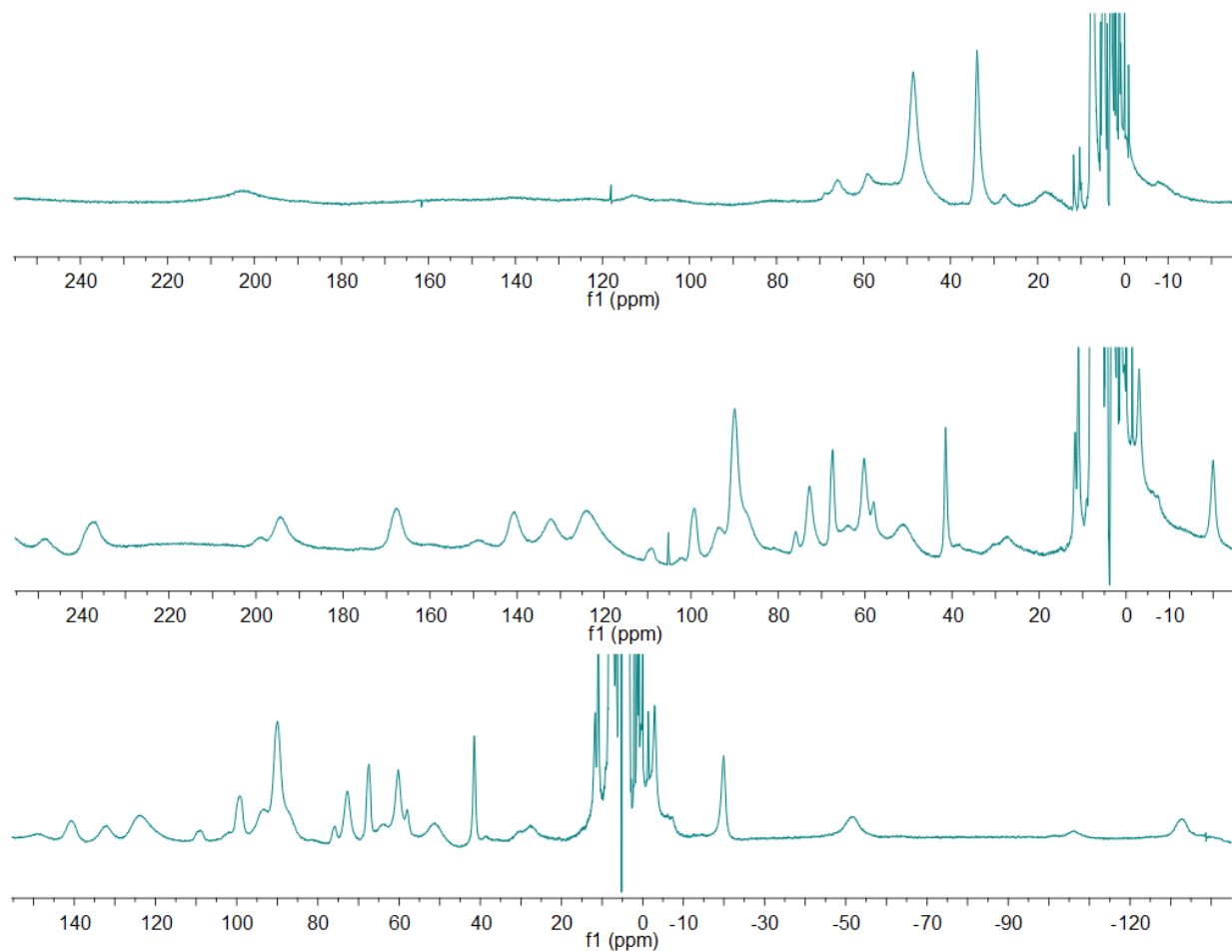


**Figure S31.**  $^1\text{H}$  NMR spectra of **1** at 295 K (top) and 213 K (middle and bottom) obtained at 300 MHz with TMS as the reference. At room temperature, no peaks are observed below -20 ppm.

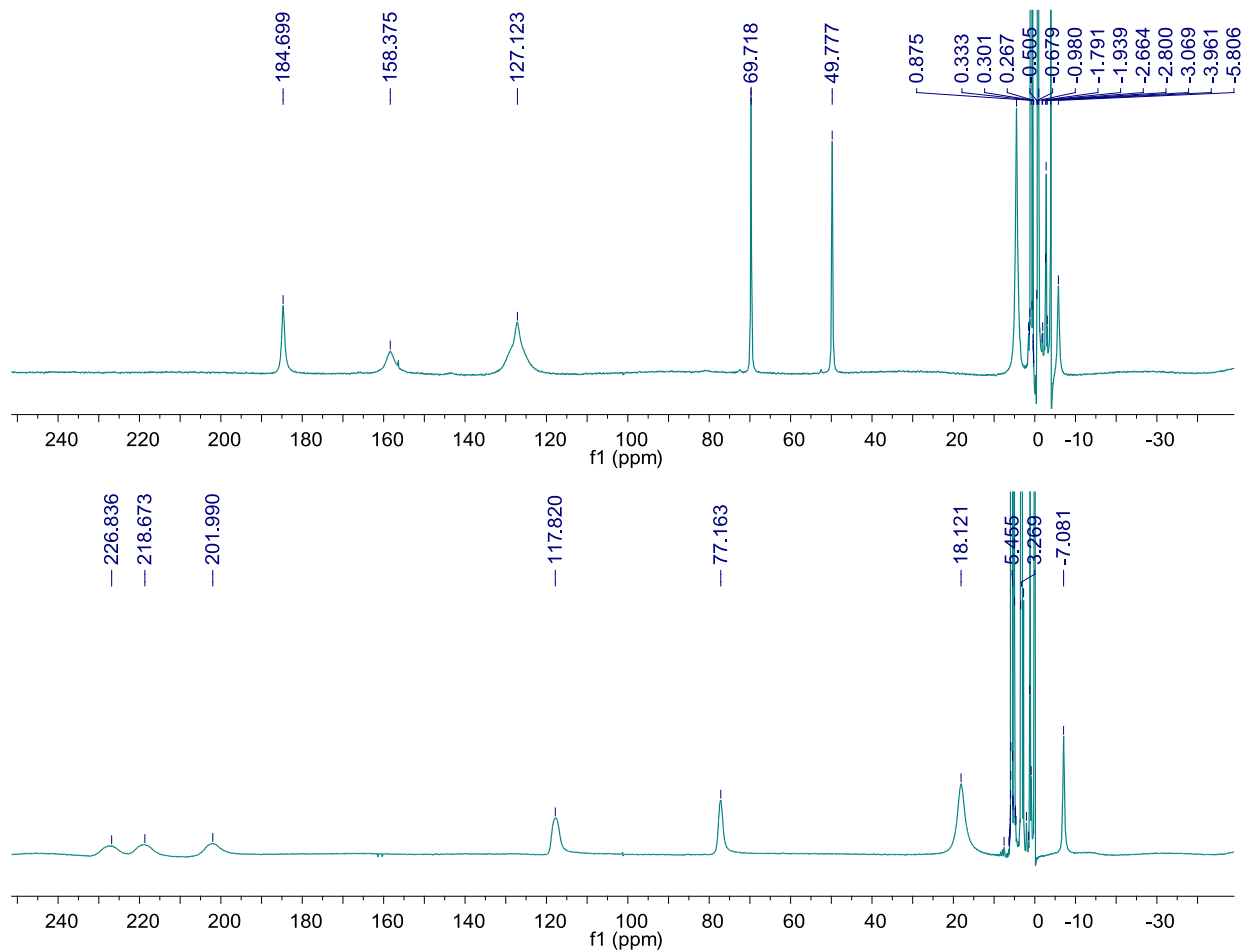


**Figure S32.** <sup>1</sup>H NMR spectra of **1** at 298 K (top) and 193 K (bottom) obtained at 300 MHz with TMS as the reference. The peak at 127.123 ppm has a small shoulder due to peak coalescence at 298 K.

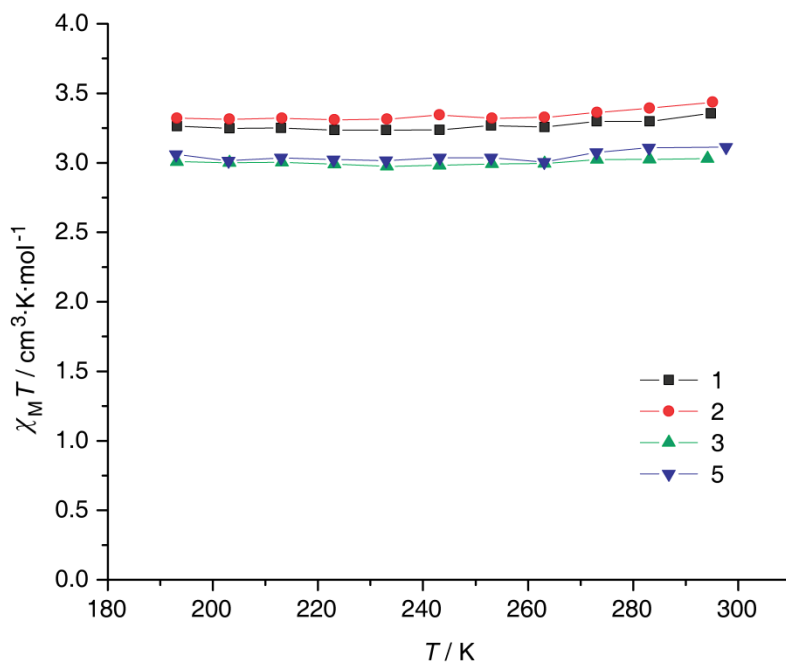


**Figure S33.** Variable temperature solution magnetic susceptibility of **1**, **2**, **3** and **5** in CD<sub>3</sub>OD using Evans' method.

*Note: At low temperatures, decreased solubility of compounds may manifest as lower-than-expected magnetic susceptibility values. The samples whose data are shown in figures S17-S20 were prepared so that they maintained complete solubility at 185 K.*